Available online at www.sciencedirect.com

ScienceDirect

Ceramics International 37 (2011) 1215–1218

CERAMICS INTERNATIONAL

www.elsevier.com/locate/ceramint

Chemical synthesis of nanosized $BaCO_3$ with a pillar-like morphology

Chen Zeng [a], Ping Li [b,c,*], HongBin Xu [b,c], ZhiFeng Xu [a], HuiHui Li [b,c], Yi Zhang [b,c]

[a] *School of Materials and Chemical Engineering, JiangXi University of Science and Technology, Ganzhou 341000, PR China*
[b] *Key Laboratory of Green Process and Engineering, Institute of Process Engineering, Chinese Academy of Sciences, Beijing 100190, PR China*
[c] *National Engineering Laboratory for Hydrometallurgical Cleaner Production Technology, Chinese Academy of Science, Beijing 100190, PR China*

Received 17 September 2010; received in revised form 29 October 2010; accepted 30 November 2010
Available online 21 January 2011

Abstract

A procedure for the preparation of nanosized pillar-like $BaCO_3$ based on the aging of barium nitrate aqueous solutions in the presence of lactic acid, sodium carbonate, and polyvinylpyrrolidone. Using X-ray diffraction analysis, scanning electron microscopy, and transmission electron microscopy, the morphological characteristics of $BaCO_3$ were controlled by altering the molar ratio of lactic acid to barium ion, as well as the initial pH and barium ion concentration. The possible formation mechanism of the nanoparticles was also discussed.

Keywords: Nanoparticles; $BaCO_3$; Lactic acid; Morphological characteristics; Oxide

1. Introduction

Nanosized $BaCO_3$ has numerous potential technological applications in pigment, optical glass, ceramic, and electric condensers thanks to its high permeability, low loss and saturation magnetization [1,2]. Various methods to synthesize this type of material have been performed, including liquid phase method [3], micro-emulsion method [4], low-temperature solid phase method [5], template method [6], and so on [7].

The liquid phase method has been widely researched because of the controllable synthesis of nanosized $BaCO_3$ with various morphologies. Organic surfactants and/or chelating ligands play significant roles in determining the morphology and size distribution of nanoparticles [8]. For example, Ma et al. [9] prepared rod-, bundle-, and flower-like $BaCO_3$ using $Ba(NO_3)_2$, $(NH_4)_2CO_3$ in the presence of organic surfactants such as cetyltrimethyl ammonium bromide (CTAB) and sodium dodecyl benzene sulfonate (SDBS). Lv et al. [10] synthesized dumbbell-, pillar-, peanut-, and ellipsoid-like $BaCO_3$ with the size of 120–400 nm by introducing citric acid (CA) as chelating ligand via a polyvinyl pyrrolidone K-30 (PVP)-assisted route. Organic surfactants such as PVP and CTAB can control crystal growth via face-selective adsorption [11], while the chelating ligands such as CA and EDTA appear to prevent both nucleation and coagulation during particle growth by shielding the barium ion [12].

This study thus aimed at preparing nanosized $BaCO_3$ using lactic acid (LA) as chelating agent via a PVP-assisted method at 25 °C. Nanosized $BaCO_3$ with a pillar-like shape was obtained by controlling the molar ratio of LA/Ba^{2+}, initial pH, and barium ion concentration. A possible mechanism for the formation of $BaCO_3$ nanoparticles was also discussed.

2. Experimental

All chemicals were analytical grade reagents and used as received without further purification. $Ba(NO_3)_2$, Na_2CO_3, PVP, and LA were dissolved in distilled water to prepare an aqueous solution. In a typical synthesis, 5 mL 0.2 M $Ba(NO_3)_2$ aqueous solution, 15 mL 100 g dm^{-3} PVP aqueous solution, and a predetermined amount of LA aqueous solution were added to a beaker under magnetic stirring for 30 min at 25 °C. The solution was then adjusted to the desired pH using 2 M NaOH. Subsequently, 5 mL 0.2 M Na_2CO_3 was added dropwise to the mixed solution under continuous stirring. White precipitate was formed during the addition of Na_2CO_3. After the reactant supply was terminated, the precipitate was left under

---

* Corresponding author at: Key Laboratory of Green Process and Engineering, Institute of Process Engineering, Chinese Academy of Sciences, Beijing 100190, PR China. Tel.: +86 10 82544808; fax: +86 10 82544808.

E-mail address: lipinggnipil@home.ipe.ac.cn (P. Li).

0272-8842/$36.00 © 2011 Elsevier Ltd and Techna Group S.r.l. All rights reserved.
doi:10.1016/j.ceramint.2010.11.046

Table 1
Morphological characteristics of the $BaCO_3$ particles precipitated by aging for different time, temperature, solutions containing variable amounts of LA and $Ba(NO_3)_2$, 0.2 M Na_2CO_3, and 100 g dm^{-3} PVP.

Sample	$Ba(NO_3)_2$	LA/Ba^{2+} mole ratio	Reaction time	Reaction temperature	Initial pH	Morphological characteristics	
						Shape	Width/length
S1	0.2 M	0	15 min	25 °C	9	Rod-like	>5 μm
S2	0.2 M	2	15 min	25 °C	9	Rod-like	200 nm/2 μm
S3	0.2 M	4	15 min	25 °C	9	Pillar-like	20–40 nm/40–80 nm
S4	0.2 M	6	15 min	25 °C	9	Pillar-like	20–50 nm/40–90 nm
S5	0.2 M	10	15 min	25 °C	9	Dendritic-like	–
S6	0.2 M	4	15 min	25 °C	13	Rod-like	50 nm/500 nm
S7	0.05 M	4	15 min	25 °C	9	Rod-like	200–300 nm/1–3 μm
S8	0.2 M	4	6 h	25 °C	9	Pillar-like	30–70 nm/50–90 nm
S9	0.2 M	4	15 min	100 °C	9	Rod-like	200 nm/2 μm

continuous stirring in its mother solution for a certain time to ensure complete equilibration. Finally, the product was separated from the solution by centrifugation, washed with deionized water and ethanol, and then dried in an oven at 60 °C overnight and collected for further characterization.

The phase of the products was analyzed by X-ray diffraction (XRD) and Fourier transform-infrared (FT-IR) spectrophotometry. The XRD analysis was carried out with a Rigaku diffractometer using CuKα radiation. The infrared spectrum was recorded by a Spectra GX FT-IR spectrometer (Perkin–Elmer, U.S.) in KBr pellets (0.002 g sample and 0.2 g KBr) with the scan number set to 8 and the resolution set to 4 cm^{-1}. The size and morphology of the products were taken using a Hitachi Model H-800. Differential thermal analysis (TGA) and differential scanning calorimetry (DSC) were performed in air atmosphere at a heating rate of 10 °C min^{-1}.

3. Results and discussion

Table 1 summarizes the effects of the LA/Ba^{2+} molar ratio, initial pH, barium ion concentration, reaction time and reaction temperature on the morphological characteristics (size and shape) of the $BaCO_3$ particles precipitated via PVP-assisted route. Through the aging of solutions with the LA/Ba^{2+} molar ratio ranging from 4 to 6, the $Ba(NO_3)_2$ and Na_2CO_3 concentrations both maintained at 0.2 M, and the amount of PVP (100 g dm^{-3}) constant, $BaCO_3$ nanoparticles with a pillar-like morphology, a mean diameter of 20–40 nm, and a length of 40–80 nm were synthesized. The morphological characteristics of the $BaCO_3$ particles were as follows: rod-like, 200 nm in width, 2 μm in length, and dendritic-like under the condition of the LA/Ba^{2+} molar ratio of 2 and 10. The rod-like particles also resulted from a high initial pH (13), low barium ion concentration (0.05 M) or high reaction temperature (100 °C), implying that the morphological characteristics of the particles were very sensitive to the reaction conditions.

The phase of all $BaCO_3$ samples synthesized in this work was confirmed by XRD and FT-IR, and all products obtained gave similar results. All peaks could be clearly indexed as a pure orthorhombic phase, which was consisted with the reported data (JCPDS card File No. 05-0378); no diffraction peaks for other phases or materials were observed in the XRD patterns. In Fig. 1a, the (1 1 1) peak was the strongest; this suggested that the $BaCO_3$ crystals obtained from the aqueous solution grew mainly along the (1 1 1) face.

The FT-IR spectrum of sample S3 is shown in Fig. 1b; this represents the characteristic absorbance of high purity $BaCO_3$. The absorption bands attributed to the vibrations of the CO_3^{2-} anion are located within the 1800–600 cm^{-1} region [13]. A weak absorption band at about 1061 cm^{-1} and at 1121 cm^{-1} as a result of the symmetric stretching vibrations were observed. The strong broad absorption centered at about 1458 cm^{-1} and a

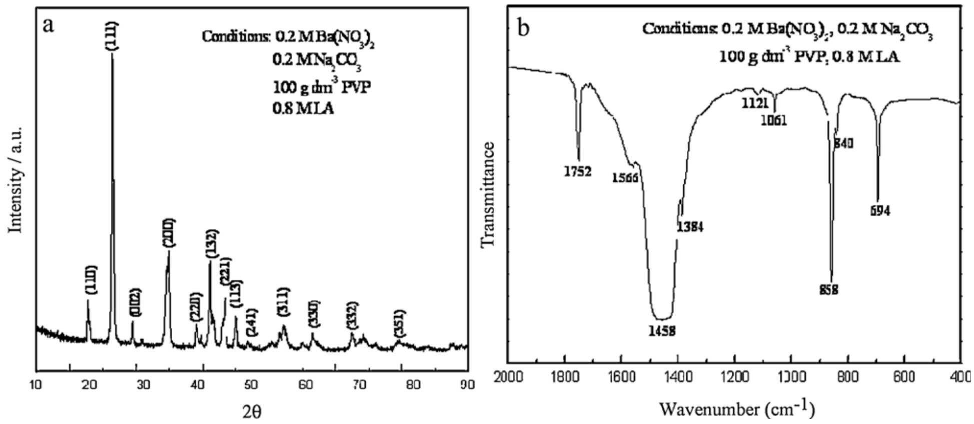

Fig. 1. XRD and FT-IR of the sample S3.

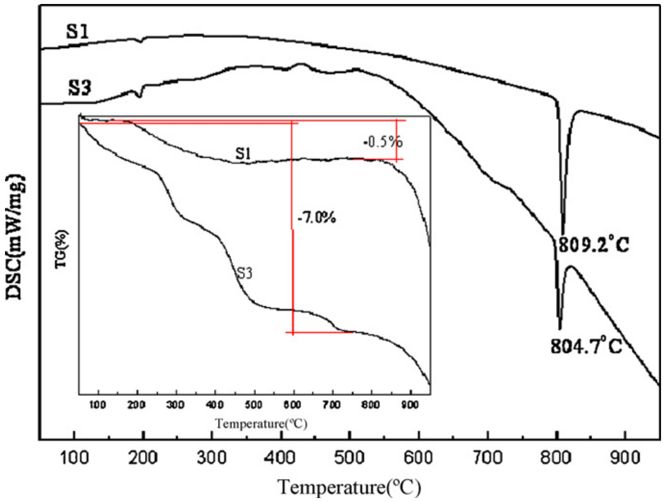

Fig. 2. DSC of the samples S1 and S3 containing the inset of the enlarged TG.

much weaker absorption at 1384 cm^{-1} were connected with the asymmetric C–O stretching vibrations; a strong sharp absorption band at about 858 cm^{-1} and at 694 cm^{-1} could be assigned to the out-of-plane bending vibrations and in-plane bending vibrations of the CO_3^{2-}, respectively [14]. In addition to these, a weak sharp absorption at about 1752 cm^{-1} could be attributed to combination of the symmetric stretching vibrations and the in-plane vibrations.

DSC and TG analysis were performed on the sample S1 and S3, and the results were shown in Fig. 2. The obtained DSC curves of the S1 and S3 revealed a weak endothermic peak at about 220 °C that was attributed to absorbed moisture. An intense endothermic peak was also observed in the DSC curve of the S1 at 809.2 °C which could be associated to the phase transition of the $BaCO_3$. This was proved by other work [15]. Compared to the S1, the TG and DSC curves showed that the S2 had the lower phase transition temperature (804.7 °C) with an associated loss weight of 7.0%, which could be attributed to the nanometer range of the $BaCO_3$ particles.

Fig. 3 shows the morphology of the $BaCO_3$ samples obtained with different LA/Ba^{2+} molar ratios. By increasing the LA/Ba^{2+} molar ratio from 2 to 10, the morphology of the $BaCO_3$ particles changed from rod-like to dendritic-like. The $BaCO_3$ particles had a pillar-like shape within the nanometer range when the LA/Ba^{2+} molar ratio was kept at the range of 4–6. The SAED pattern of sample S3 (Fig. 3e) indicated the single-crystalline structure of the nanoparticles and the preferential growth direction of the pillar along the [1 0 0] zone axis of the $BaCO_3$. Without LA addition, the $BaCO_3$ particles had a rod-like shape with diameters of several hundred nanometers and lengths of several micrometers. The formation of the $BaCO_3$ rod was reported to result from the aggregation of nanoparticles, which was related to the oriented attachment mechanism [16]. With the addition of LA, the LA that reacted with the Ba^{2+} ion to form the Ba–LA complex provided a polymeric network that hinders cation mobility. Once the LA was dissociated from the Ba^{2+} ion, it bound to the specific surface of the precipitated $BaCO_3$. This implied that the LA tailored the micron-sized $BaCO_3$ rods to obtain the pillar-like $BaCO_3$ nanoparticles.

However, with the addition of excessive LA (LA/Ba^{2+} molar ratio = 10), the $BaCO_3$ particles had a dendritic-like shape, which was responsible for certain facets resulting from the excessive Ba–LA complex. The Ba-LA complex included $Ba(LA)^+$ and $Ba(LA)_2^0$ ions[17]. The $Ba(LA)_2^0$ ion became dominated with the excessive LA addition. Once the LA was dissociated from the Ba^{2+} ion, the $Ba(LA)_2^0$ ion released two LA ions; two specific facets with different orientation would be produced. It could be supposed that the dendritic-like $BaCO_3$ formation was related to the different oriented facets.

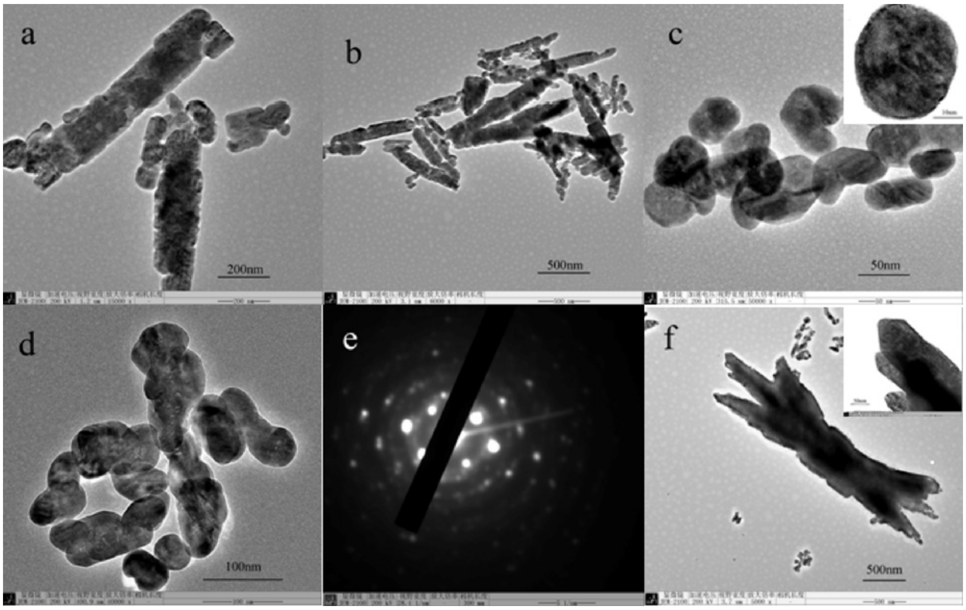

Fig. 3. SEM photograph of S1 (a), TEM images of samples S2 (b), S3 (c) containing the inset of the enlarged TEM image, S4 (d), S5 (f), SAED pattern of the S3 (e).

4. Conclusions

Chemical synthesis of nanosized $BaCO_3$ with a pillar-like morphology and a possible mechanism were investigated, leading to the following conclusions:

(1) $BaCO_3$ nanoparticles with a pillar-like shape could be obtained in an aqueous solution containing Ba–LA complex, which tailored the aggregation to form the $BaCO_3$ nanoparticles.
(2) The LA/Ba^{2+} molar ratio, initial pH, and barium ion concentration were found to have close relations with the morphological characteristics of $BaCO_3$ particles.

This preparation method reported herein was simple, low-cost and suitable for large scale production of the pillar-like $BaCO_3$ nanoparticles.

Acknowledgements

This work was financially supported by the National Basic Research Program (973 Program) of China (No. 2007CB613500), and the National Nature Science Foundation of China (No. 50904058).

References

[1] L. Chen, Y.H. Shen, A. Xie, et al. Cryst. Res. Technol. 9 (2007) 886.
[2] L.L. Li, Y. Chu, Y. Liu, L.H. Dong, L. Huo, F.Y. Yang, Mater. Lett. 60 (2006) 2138.
[3] V.K. Lamer, R.H. Dinegar, et al. J. Am. Chem. Soc. 72 (1950) 4847.
[4] K. Christo, M. Dafina, Chem. Eng. Process. 44 (2005) 115.
[5] H.W. Hou, X.Q. Xin, S. Shu, Coord. Chem. Rev. 153 (1996) 25.
[6] Y.H. Gao, H.L. Niu, Q.W. Chen, Chin. J. Inorg. Chem. 19 (2003) 37.
[7] M.A. Alavi, A. Morsali, Ultrason. Sonochem. 15 (2008) 833.
[8] L. Gao, J. Sun, Y.Q. Liu, Dispersion and Surface Modification of Nanopowders, Chemical Industry Press, Beijing, 2003.
[9] M.G. Ma, Y.J. Zhu, G.F. Cheng, Y.H. Huang, Mater. Lett. 62 (2008) 3110.
[10] S. Lv, J. Sheng, S. Zhang, W.D. Sun, Mater. Res. Bull. 43 (2008) 1099.
[11] S.H. Yu, H. Cölfen, K. Tauer, M. Antonietti, Nat. Mater. 4 (2005) 51.
[12] T. Sugimoto, Adv. Colloid Interface 28 (1987) 65.
[13] C. Rey, B. Collins, T. Goehl, I.R. Dickson, M.J. Glimcher, Calcified Tissue Int. 45 (1989) 157.
[14] S. Poonam, H.S. Virk, Open Surf. Sci. J. 1 (2009) 34.
[15] Y.Q. Xue, Q.S. Zhao, C.H.J. Luan, Colloid Interface Sci. 243 (2001) 388.
[16] R.L. Penn, J.F. Banfield, Geochim. Cosmochim. Acta 63 (1999) 1549.
[17] R.M. Smith, A.E. Martell, Critical Stability constants, Plenum Press, New York, 1979.